# Assessment of the influence of façade location and orientation in indoor environment of double-skin building envelopes with perforated metal sheets

J.M. Blanco[a,], A. Buruaga[a], J. Cuadrado[b], A. Zapico[c]

[a] Fluid Mechanics Department, School of Engineering, Building I, University of the Basque Country, UPV/EHU, Plaza Ingeniero Torres Quevedo, 1, 48013, Bilbao, Spain

[b] Mechanical Engineering Department, School of Engineering, Building I, University of the Basque Country, UPV/EHU, Plaza Ingeniero Torres Quevedo, 1, 48013, Bilbao,Spain

[c] Energy Department, School of Engineering, East Wing, University of Oviedo, Campus de Viesques s/n, 33271, Gijon, Spain

ABSTRACT

Double-skin perforated sheet façades, enclosures consisting of perforated screens, air chambers and glass/wall sheets, are features of modern building design that are winning greater acceptance. A detailed analysis of their suitability across Europe is first performed here. A reference building both with and without the protective double-skin perforated sheet envelope is subjected to a comparative test of solar energy gains with regard to the environment. Additionally, the results of a preliminary survey are presented on the visual perceptions of different patterns of perforated metal sheets. Then the behaviour of these configurations is addressed, through a complete "Energyplus® model" (design builder). A test campaign on a reference perforated screen mounted on a service building of reference was fully monitored over one year, supported by thermographic data recorded for additional validation purposes during the same period. The new parametric energy assessment takes additional variables into account, such as orientation and location of the façade, demonstrating that the real performance for such enclosures greatly depends on them. Accordingly, the influence of different combinations of perforated screens on cooling, heating and lighting loads demonstrates the suitability of a previously optimized configuration in terms of relative energy savings.

## 1. Introduction

Nowadays, the indoor environmental quality in buildings is assuming greater importance [1], due to the need for efficient energy performance in an emerging scenario where the key issue is now the climate change. The use of perforated metal screens as a protective skin in façades can be very useful for this purpose [2,3]. Over recent years,the behaviour of double-skin façades has been highlighted in residential buildings with such methods as technological enclosures with passive thermal control [4], solar façades [5], dynamic windows [6], andnaturally ventilated façades [7,8]. Solar shading control strategies foroffice buildings represent another important factor in the visual impact on its occupants [9–11]. Other studies have focused on shading and its impact on energy savings [12–14].

As other parameters, the control of materials used in the double skin façades is crucial to evaluate the behaviour accurately. A great number of studies have been carried out around this. With metal façades theeffect of the aging (life cycle assessment) over the metal plates has been studied [15] whereas wood has been considered to increase the energy efficiency [16,17]. Even walls with living vegetation [18,19] and even applied to hot arid climates [20] have been fully addressed. Anyway, as important as material, is the use of sustainable energies aiming to reduce the fuel energy consumption [21–23].

Another key issue is the use of different sized perforations to depict images and graphics, which provides an original and individual boostfor residential, public and commercial buildings [24]. But the use of different perforation sizes merely for displaying a particular image, such as a corporative logo, can further complicate any evaluation of energy savings.

Other inputs such as airflow analysis have also been implemented [25]. Nowadays, full monitoring and CFD simulations of the air flow in the external cavity of double-skin façades (air chamber between the internal wall and the perforated sheet) has also been addressed [26].

The people living or working in these buildings have voiced their concerns over the use of perforated screensin several directions, such as in terms of fire safety, as in case of fire outbreak inside the building, the sheets represent a robust barrier for those users trying to escape but alsofor firemen trying to extinguish it, as also contribute to the vertical propagation of both smoke and fire within the chamber, according to the International energy Agency (IEA), Energy Conservation in Buildings and Community Systems (ECBCS), Annex 44 [27]. To solve this issue the implementation of fire exits has been discussed. Another relevant concern is the visual perception of users. A preliminary analysis on the visual influence on their daily life was therefore also performed here, through a survey administered to a population of 100 people (students and staff) on university campuses, participating also building developers, architects and even visitors.

The behaviour of enclosures made of perforated metal sheets at different orientations and locations with rather different weather conditions among them will be examined in depth. The study will be presented in two main sections:

In a first section of the study, enclosures and such behaviour in different capitals across Europe will be studied with the "Ecotect" software package [28]. A recognized environmental analytical tool, designers use it to simulate building performance from the earliest stages of conceptual design. The aim here is to demonstrate the convenience of the enclosure

system by location.

In the second section, a detailed case study of load consumptions was performed at two representative locations in Spain; rotations around the four cardinal directions are proposed, in an analysis of enclosure behaviour, depending on the spatial orientation of the façade, with the "Design Builder" software package, powered by EnergyPlus [29], evaluating the optimum perforation rate for each orientation, as a parametric study

The same material (galvanized steel) for all the orientations has been studied, but different perforation rates (p) (100, 70, 55, 40, 25 and 10%) were analyzed. The percentages refer to the ratio of open surface over the total metallic surface area of the panel. Here, the aim is to examine their respective responses in different orientations, in order to choose the best configuration for each orientation but also location (climate area): while 100% tells us there is no sheet, 10% represents a conceptual design limit.

The Energy Plus model processed all data from the monitoring of a south-oriented metal perforated screen of a university building, throughout an extensive one-year test campaign in Bilbao (northern Spain). Metal sheet temperatures were monitored at different points uniformly distributed across the whole surface, building up a detailed behaviour of the double skin façade. External weather conditions, such as temperature, humidity and wind speed were measured at a weather station on the roof of the building and several hot wire anemometers together with air temperature probes were also located, to evaluate the movement of the air inside the 0.7 m width air chamber.

An Infrared thermography (IRT) study was also implemented, to reinforce the experimental validation procedure, matching the previous results. IRT is the science of detecting infrared energy emitted from an object, and displaying the result as an infrared image [30,31]. These cameras capture a general view of the thermal behaviour of the façade, with no direct contact with the test material. Thermal information may therefore be captured with equipment operating at a safe distance away, with a better chance of distinguishing temperature anomalies under normal operating conditions through a general view of the façade, and not only at a specific point, as with a thermal sensor. The noncontact nature of infrared cameras makes it ideal for a wide range of applications difficult to reach such as detecting energy-related problems in building envelopes [32,33].

As a result, the case study performed in Spain was in two different climate areas, represented by two cities: Bilbao in the north climate zone I, characterized by fresh and humid weather conditions with low solar irradiance factors ($Ir \leq 3.8$ kW h/m$^2$ day) and Seville, in southern Spain (climate zone V, characterized by severe hot and dry conditions, with high solar irradiance factors: $Ir \geq 5$ kW h/m$^2$ day). For all of them, the total energy consumption of the building was split into heating, refrigeration and illumination loads. Regarding the latest, electric lighting depends on daylight illuminance level in a zone which is defined according to many factors, including sky condition, sun position, location, size, and glass transmittance, window shades and reflectanceof interior surfaces.

The energy gains for each configuration were compared with those from a reference façade (without any additional protective skin on it), for these two different locations. The façade orientations were finally characterized by all eight combinations of the main cardinal directions(N, NE, E, SE, S, SW, W and NW).

## 2. Aims and methodology

The main goal of this investigation is to study the behaviour of perforated metal sheets placed on façades as external enclosures, at different locations and at various orientations, so as to evaluate their environmental effects in terms of energy savings.

A preliminary study of visual impressions will also be presented through a survey, analysing the opinions and concerns of people who have looked through a window at 6 different samples of perforated sheets with different patterns (based on perforation rates and separations between holes).

Subsequently, a detailed analysis at 18 different European locations will be performed with "Ecotect®" software, so as to obtain a comparative test of energy gains, with and without the protective doubleskin perforated sheet envelope. From among them all, the incidental solar energy gain on a south-oriented façade will be analysed as the worst-case scenario.

Aiming to arrive at an accurate evaluation of the behaviour of such screens with different orientations, according to their cardinal directions, different perforation rates were used to evaluate the optimum configuration for each location and orientation, at all times considering the same material (galvanized steel) for comparative purposes. This study was performed with "Design Builder®" and the total energy consumption and savings per year for the different cases were split into "illumination", "heating" and "cooling" gains respectively, as a useful insight indeed for building developers.

Finally, the whole experimental validation procedure was addressed through the complete monitorization of a real façade using the last generation of weather stations and temperature probes, together with a full data acquisition system, recording a wide historical set of inputs and complemented through an experimental analysis based on the Infrared thermography technique, thereby reinforcing the validation procedure, so a case study was finally addressed.

## 3. Preliminary analysis on the visual aspects of perforated sheets

Occupant productivity in commercial buildings such as offices is a key concern that depends on the indoor environment quality [34,35]. It has been measured through surveys to determine visual comfort from those occupants [36–39].

A survey was administered to more than 100 engineering students, designers, architects and visitors at different Engineering Schools in Spain. Six different patterns of metallic perforated sheets (1 m heightand 0.5 m width) were mounted together alongside an open window as shown in Fig. 1a. The criteria used to select the Surveyees were the population that had to live with this type of envelopes most of theirdaily life, so first of all students were selected, followed by designersand architects whose decisions on this matter are usually based on thermal constraints rather than in visual aspects and finally casual visitors. The 85% of the population of the survey were students, followed by 13% of casual visitors and the remaining 2% of designers. Their opinions did not differ very much from each collective, even considering for some cases their relevant difference in age and optical capacities. Surveyees were asked to assess the pattern that seemed to facilitate better observation of the exterior of the building when theobserver was standing at either a short (1 m) or a long distance (5 m) away. The full definition of the patterns which are the most commonly used in the study are shown below in Table 1, for three different perforation rates (p), as centred in the range of commonly used. The pattern formed between centres (L) and diameter of the holes (D), was demonstrated that directly affects the visual perception across perforated sheets [40,41]. Fig. 1b shows the results of the tests. It can be seen that sample 3

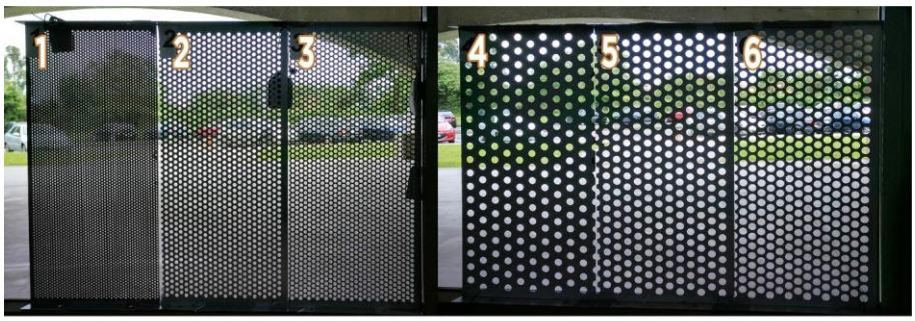


a)

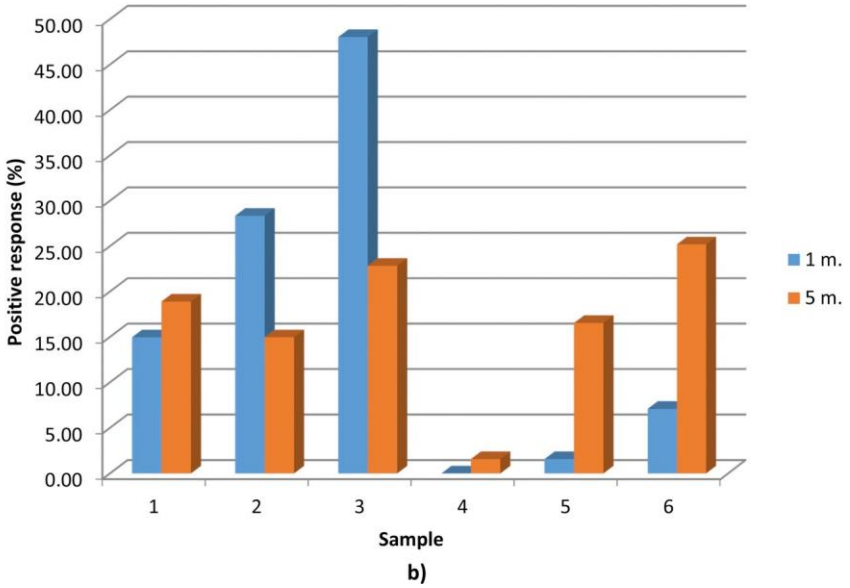


b)

**Fig. 1.** Visual perceptions of perforated metal sheets carried out through a survey, (a) experimental assembly, and (b) results obtained for observers situated at two different distances

**Table 1**
Main characteristics of the six patterns of perforated sheets used for the visualtest

| Sample | Denomination | Quincunx layout | L (mm) | D (mm) | p (%) |
|---|---|---|---|---|---|
| 1 | D2 L4 AL | 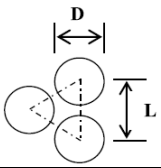 | 4 | 2 | 25 |
| 2 | D5 L8 GAL | | 8 | 5 | 35 |
| 3 | D5 L7 GAL | | 7 | 5 | 40 |
| 4 | D10 L2O GAL | | 20 | 10 | 25 |
| 5 | D10 L16 GAL | | 16 | 10 | 35 |
| 6 | D10 L14 GAL | | 14 | 10 | 40 |



It was the most positively assessed by the observers standing a short distance away (1 m), while sample 6 was considered

the best valued at a longer distance (5 m) away closely followed by sample 3. The results indicated that the patterns with smaller hole diameters were considered better at the shortest distance. As the distance increased, the perceptions of the different patterns became more uniform, except for sample4 which was the worst valued for both situations, while the best globally valued pattern was sample 3.

## 4. Convenience of the implementation of such enclosures basedon energy savings across Europe

### *4.1. Model definition*

Ecotect® is a widely used software for the thermal analysis of buildings. By simulating the position of the sun, this package performs the calculation of different energy gains, throughout the day. The output is the sum of the daily energy gains on an annual basis (Wh/m2 year). It manages data from the US energy department, to obtain the weather averaged values, [29]. The data are originally obtained in "IWEC" (International Weather for Energy Calculations) format, exported later as "EPW" (EnergyPlus Weather) format, and converted into "WEA" (Weather Ecotect Analysis) format, for their final management. Weather data include the solar hours, rain intensity and humidity together with other parameters. Among them the so called "clouding factor" directly influences the amount of solar energy gained by the building. This factor is included in the IWEC format file related to a specific place, which has been previously calculated on site, estimating the filtering of sunlight made by the clouds, pollution or other atmospheric elements. This value is variable during different parts of the day and/or the year.

**Table 2** Boundary conditions for the definition of the Ecotect® model for all the locations.

| Ecotect parameters | Value |
|---|---|
| Available energy | [W h $m^{-2}$] |
| Average shade | % |
| Reflected energy | [W h $m^{-2}$] |
| Incident solar radiation | [W h $m^{-2}$] |
| Total Incident solar radiation | [W h ] |
| Absorbed energy | [W h $m^{-2}$] |
| Total Absorbed energy | [W h ] |

In this case, the modelling of a reference enclosure unit,(10 × 8 × 3.5 m) prismatic volume is shown for comparative pourposes, so for the south-oriented side (10 × 3.5 m) representing the screen, a glass wall was defined as depicted in Fig. 2. As a shade device,a 1 cm thick galvanized steel sheet, with 5 mm diameter perforations in quincunx layout at a distance of 7 mm between the centres meaning ap = 40% was implemented (the best valued configuration previously obtained from the visual perception analysis, named "sample 3"). The air gap was e = 0.7 m, while Table 2 shows the boundary conditions requested for all the locations under consideration, as will next be explained in detail.

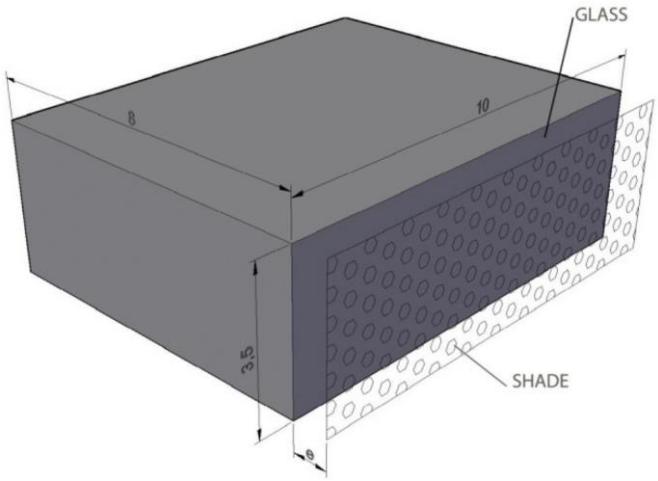


**Fig. 2.** Ecotect® model definition, volume of study

**Table 3** Thermal and geometric parameters for galvanized steel sheets for different perforation rates

| Parametric values | Definition | (p = 10%) | (p = 25%) | (p = 40%) | (p = 55%) | (p = 70%) |
|---|---|---|---|---|---|---|
| (a) Radiant parameters: | | | | | | |
| Solar transmittance | $\tau$ [$^0/_1$] | 0.1 | 0.25 | 0.4 | 0.55 | 0.7 |
| Solar reflectance | 1-$\tau$-$\alpha$ (1-p) [$^0/_1$] | 0.333 | 0.2775 | 0.222 | 0.1665 | 0.11 |
| Thermal hemispherical emissivity | $\varepsilon$ (1-$\tau$) [$^0/_1$] | 0.117 | 0.0975 | 0.078 | 0.0585 | 0.039 |
| Thermal transmittance | $\varphi$ [$^0/_1$] | 0.15 | 0.19 | 0.38 | 0.45 | 0.82 |
| (b) Air space parameters: | | | | | | |
| Shade to glass distance | e [m] | 0.70 | 0.70 | 0.70 | 0.70 | 0.70 |
| (c) Other parameters: | | | | | | |
| Sheet thickness | K [m] | 0.01 | 0.01 | 0.01 | 0.01 | 0.01 |
| Sheet conductivity | $\lambda$ [W $m^{-1}$ $K^{-1}$] | 50 | 50 | 50 | 50 | 50 |

*4.2. Approach to efficiency assessment*

Different European locations were selected for this preliminary study, distributed between latitudes 35° and 65° and represented here by just 18 relevant cities, from Nicosia in the south to Rekjavik in the north, as depicted in Fig. 3a.

It is important to point out that the result obtained is the transmittance through the perforated screen not the internal energy gain, which will be analysed in depth in the second section of this study.

The comparative test showing the energetic contribution (Wh/m2year) to our reference enclosure unit with and without the protective cover provided by the perforated metal sheets is depicted in Fig. 3b. As can be clearly noted, the behavior according to the latitude presents a noticeable inflection point around the 55° parallel, in both scenarios. The reasons for this inflection point around these locations for both scenarios is simply the evolution of the climatic conditions from hot to cold areas, so the more severe the conditions are, the greater the energetic influence of the metal sheets. The most important outcome is that the implementation of the perforated metal sheet heavily mitigates these solar energy gains. It can be read both in terms of latitude orientation, and especially with regard to the absolute global values when implementing these constructive solutions, clearly demonstrating the relevance of their use, especially for warmer countries, at lower latitudes.

An accurate evaluation of the behaviour of such screens in terms of orientation will now be described below, with a view to a greater optimization.

**Table 4** Radiative properties, (a) metal sheet, and (b) glass sheet.

| Radiative properties adopted | $\alpha$ [$^0/_1$] | $\varepsilon$ [$^0/_1$] | $\tau$ [$^0/_1$] | r [$^0/_1$] |
|---|---|---|---|---|
| Clean metallic galvanized sheet | 0.65 | 0.13 | 0.19 | 0.16 |

**Fig. 3.** European locations selected for the preliminary study (a) distribution between parallels 35°and 65°, and (b) comparative energy gains with and without the respective perforated sheet envelope

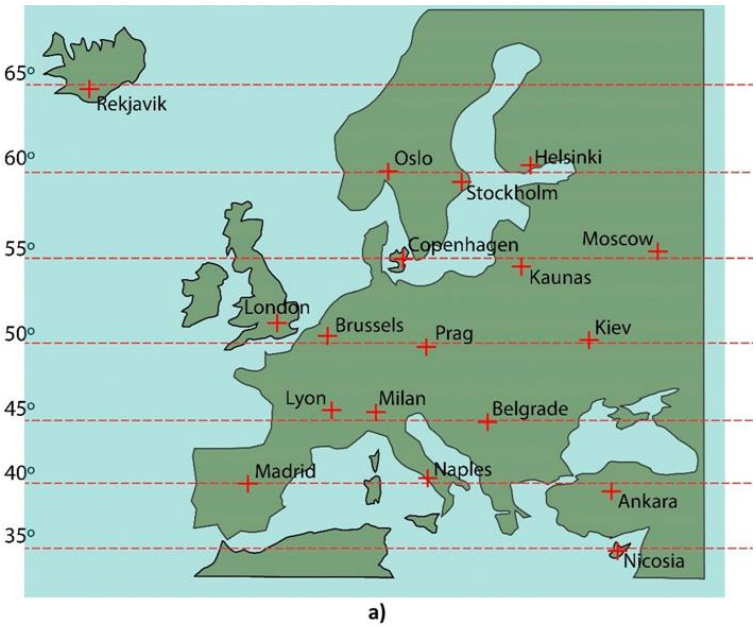


a)

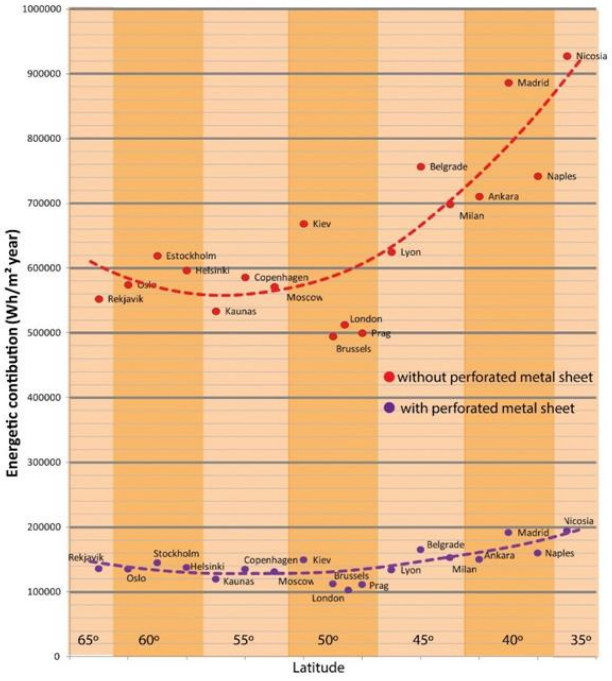


b)

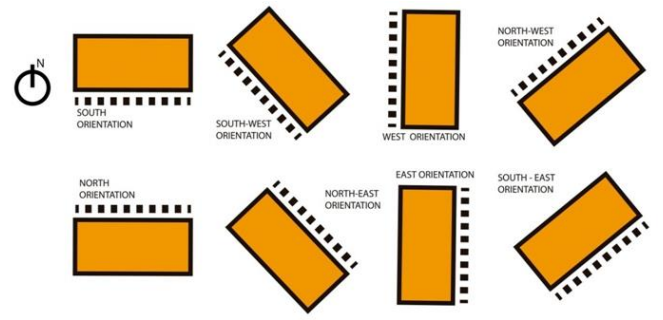


a)

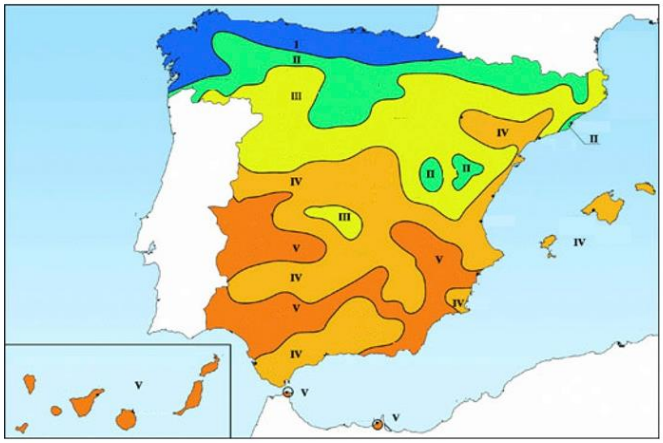

*Courtesy Spanish Technical Code*

| CLIMATIC ZONE | I | II | III | IV | V |
|---|---|---|---|---|---|
| AVERAGED IRRADIATION (KWh/m² day) | < 3.8 | 3.8 - 4.2 | 4.2 – 4.6 | 4.6 - 5.0 | > 5.0 |

b)

**Fig. 4.** Study regarding orientations and locations, (a) different combinations of cardinal directions and (b) climate zones in Spain (Source: Spanish Royal Decree Q 14/2010).

## 5. Assessment on façade orientation

### *5.1. Energy Plus® model definition*

The Design Builder® software, (powered by Energy Plus®) is used in this analysis, due to having fully demonstrated its potential to obtain the optimum parameters of the perforated sheets, aiming to assessing energy savings [42–44].

There are three available shading device options: “shade”, “blind” and “screen” [45–48]. Shades are perfect diffusers while reflective properties of blinds vary according to solar angle of incidence. For this research, the “screen” type has been selected, because it consists of intersecting orthogonally-crossed cylinders, the surface of which it is assumed are diffusely reflecting. Three types of thermal interactions are considered in the window shading device; the interaction between the shading layer and the adjacent glass, between shading layer and the room in the case of interior shading and finally between the shading layer and the outside surrounding in the case of exterior shading.

The convection of the airflow between the shading element and the glass is also considered. This flow affects the temperature of the glazing and shading elements and is determined on the model described in the ISO Standard 15,099 [49]. The boundary conditions of the exterior shading device can be summarized as follows:

The long-wave radiation (Ir) is absorbed by the shading device from the surrounding, or transmitted by the shading element and absorbed by the adjacent glass.

Both direct and diffuse solar radiations are absorbed by the shading device.

A buoyancy effect induces natural convective airflows into the space between the shading device and the glass, affecting the convection coefficients of shading-to-gap and glass-to-gap interactions

The heat transfer coefficient [50] is calculated in Design Builder® aseq. (1):

$$h_{cv} = 2h_c + 4v$$

where “$v$” represents the average air speed inside the chamber.

Screen transmittance [51] of the diffuse radiation value was computed as the integrated average of the combined

beam transmittance over the directions of incidence using spherical coordinates ($\theta$, $\Phi$), in which the z-axis was perpendicular to the plane of the screen, as shown in eq. (2):

$$T_{SC}^{dif,dif}(\gamma, \rho_{SC}) = \frac{\sum_{j=i}^{N}\sum_{i=1}^{M} T_{tot}(\gamma, \rho_{SC}, \theta_j, \varnothing_i)\sin(\theta_j)\cos(\theta_j)}{\sum_{j=i}^{N}\sum_{i=1}^{M}\sin(\theta_j)\cos(\theta_j)}$$

where, the total temperature is defined by eq. (3) as the sum of twocontributions in terms of relative solar angles:

$$T_{tot}(\gamma, \rho_{SC}, \theta_j\varnothing_i) = T_{beam}(\alpha', \phi') + T_{scatt}(\alpha', \phi')$$

Screen reflectance (overall value for the screen assembly, accounting for the screen material itself and the open spaces between the screen materials) was calculated by first subtracting the direct-todirect screen transmittance from the incident beam, which approximates the fraction of incident beam solar radiation striking the screen that is not inwardly transmitted as a function of the relative angles of incident radiation as shown in eq. (4):

$$R_{SC}^{dir,dif}(\alpha', \phi') = \rho_{SC}(1 - T_{SC}^{dir,dif}) - T_{SC}^{dir,dif}$$

The screen absorptance (overall value for the screen assembly, accounting for the screen material itself and the open spaces between the screen materials) was calculated as the quantity of the unit incident flux minus the screen transmittance previously defined in Equation (2) multiplied by the diffuse absortance of the screen material, as shown in eq. (5):

$$A_{SC}^{dir}(\alpha', \phi') = (1 - T_{SC}^{dir,dif})(1 - \rho_{SC})$$

The reference enclosure unit is coincident with the one previously studied with Ecotect® and depicted in Fig. 2 for comparative purposes, consisting of a 10 m wide, 3.5 m high, and 8 m deep volume, equipped with a 3.5 × 10 m south oriented glass façade. The perforated metal sheet protection was implemented over the glassscreen, permitting a fixed air gap (convection chamber) in between of 0.7 m. This enclosure unit of reference was later replicated to be adapted to the real dimensions of the building of reference, which will be described next.

The general thermal characteristics of the Design Builder® model are shown in Table 3, while Table 4a shows the irradiative characteristics of the perforated galvanized sheet panel, and Table 4b shows the characteristics of the double glass sheets.

Regarding the façade orientations, Fig. 4a, shows the differentcombinations of cardinal directions such as (N, NE, E, SE, S, SW, W and NW) that were studied, and finally, regarding locations, two representative cities in Spain were chosen: Bilbao in the North (climate zone I) and Seville in southern Spain (climate zone V), as defined in RD 2429/1979 [50]. Fig. 4b depicts the various climate zones that are defined in Spain, with their respective values of averaged irradiation ($I_r$).

### *5.2. Experimental procedure and validation*

A south-oriented metal perforated screen of the modern nine-storey building II corresponding to the School of Engineering, University of the Basque Country in Bilbao (northern Spain), as can be seen in Fig. 5a, was fully monitored throughout a complete year, as part of an intensive measurement campaign, for the validation of the previously presented EnergyPlus® model. The whole façade is composed of rectangular perforated sheets made of galvanized steel, each one measuring 3.5 × 1.5 $m^2$, with a standard perforation rate of p = 40%, chosen as a basic standard rate for the experiments.

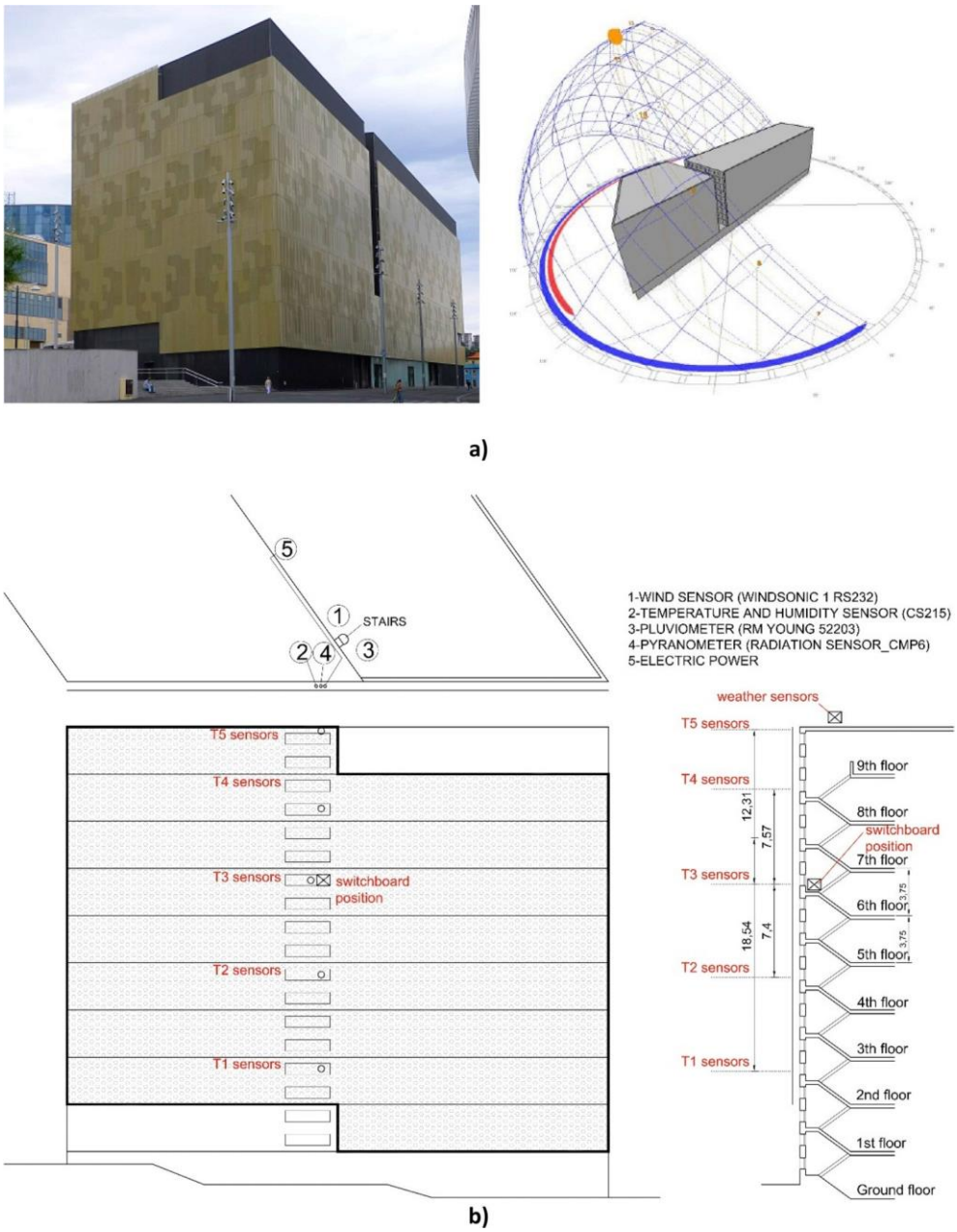


**Fig. 5.** Case-study for validation purposes, (a) picture of the south-oriented façade and (b) position of the temperature probes, anemometers and weather station

Schematic layout of the measurement equipment is depicted in Fig. 5b. Metal sheet temperatures are monitored by means of pt100 temperature probes (AISI 316) at five levels, uniformly distributed throughout the whole surface, attached to a specific thermal adhesive paste, while the data acquisition system equipped with a Campbell Scientific CR1000 data logger with the AM16/32 multiplexor and a module for compact flash cards (CFM 100) placed in an ENC 16/18 switchboard weatherproof box (protection class IP66) was fixed between the 6th and the 7th floors. External weather conditions, such as temperature, humidity, solar radiation and wind speed are monitored through a weather station, placed on the roof, the elements of which are depicted in Fig. 6a, Kipp & Zonen Pyranometer model CMP-6, a WindSonic model (1405-PK-021) with a RS 232 output, exterior temperature and relative humidity sensor, model CS215 and Rain gauge: RM Young, model 52,203. Besides, several hot wire anemometers (AM4204MA) were also located at different levels throughout the façade gap, (Fig. 6b left and right respectively), in order to account for the air conditions inside the 0.7 m air chamber. More precisely, these anemometers were placed on the 2nd, 4th and 6th floors of the building and for each one of them at the three axes with regard to the wall, in the cross section of the gap, measured from the façade towards the perforated metal sheet at 10, 35 and 60 cm respectively.

The main technical features of the abovementioned equipment including the data acquisition system are summarized in Table 5.

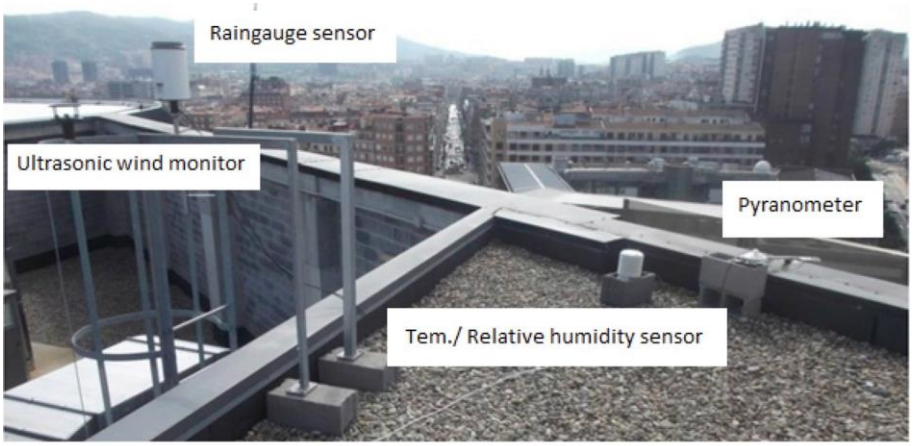


a)

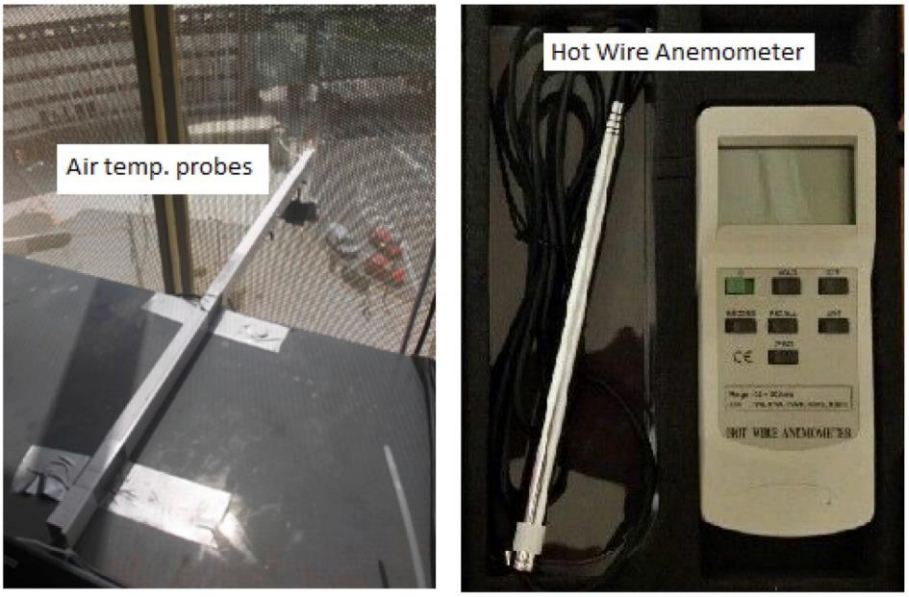


b)

**Fig. 6.** Detail of the data acquisition system, (a) weather station, placed on the building roof and, (b) detail of air temperature probes and hot wire anemometer

**Table 5** Main features of the equipment including data acquisition system

(a)

| | DG Clr. 6mm/13 mm air |
|---|---|
| U-value [W $m^{-2}$ $K^{-1}$] | 2.708 |
| Total solar transmittance [$^{0}/_{1}$] | 0.697 |
| Direct solar transmittance [$^{0}/_{1}$] | 0.604 |
| Light transmittance [$^{0}/_{1}$] | 0.781 |

(b)

| Equipment | Model | Range | Accuracy |
|---|---|---|---|
| METAL SHEET TEMPERATURE: | | | |
| Temperature probes (AISI 316) | Pt100 | - 50 to + 180 °C | ± 0.5% (full scale). |
| ENVIRONMENTAL: | | | |
| Pyranometer (Kipp&Zonen) | CMP-6 | 285–2800 nm solar radiation | 5–20 μV/W/$m^2$ |
| Ultrasonic wind monitor (RS232) | 1405-PK-021 | 0–60 m/s/0-359° | ± 0.01 m/s |
| Temp./Relative humidity sensor | CS215 | - 20 to +60 °C/0–100% RH | 0.01 °C/0.03% RH |
| Raingauge sensor (Young) | 52,203 | 200 $cm^2$ catchment area | 2% up to 25 mm/h |
| Hot wire anemometer | AM-4204HA | 0.2–20.0 m/s | ± 1% (full scale) |
| DATA ADQUISITION SYSTEM: | | | |
| Data logger (Campbell Scientific) | CR1000 | 1 CS I/O, 1 RS-232, 1 | 0.33 μV |
| Multiplexor | AM16/32 | 9.6 to 16 Vdc | 1 m |
| Compact flash cards module | CFM100 | 200–400 kbits $s^{-1}$ | – |
| Weather-proof box (Switch board) | ENC 16/18 | – | – |

The evolution of the values obtained in the monitoring process such as the chamber air speed, metal sheet temperature and external conditions (exterior and metal sheets temperatures, exterior and chamber air speed and solar radiation) for a summer day type are depicted in Fig. 7a. The day chosen for the presentation of the results was that on which the highest thermal radiation levels were recorded. In the course of that day of reference, peak radiation levels of over 950 $W/m^2$ were measured between 14:00 and 16:00 p.m. The ambient temperature hit33 °C around midday and remained with small fluctuations until around 17:00 p.m. It should be mentioned that ambient temperatures of up to36 °C were measured on different summer days, although at lower solar radiation levels.

Increases in the temperature of the perforated metal sheet were mainly due to radiation loads. In turn, it heated the air inside the chamber, raising the convection coefficient and subsequently the vertical speed of the air in the gap. The airflows slightly decreased the metal sheet temperature, (some fluctuations can be appreciated in the graphic) in the time gap between 11:00 a.m. and 14:00 p.m. where the vertical air speed in the chamber was higher. EXterior wind was also partially responsible for temperature decreases in the metal sheet.

A specific configuration reported in Fig. 7b was selected, to showthe evolution of the metal sheet temperatures obtained both throughthe Design Builder model (DB) and through experimental measurement (EXP), and thereby validate the model. Relevant matching can be appreciated between temperatures recorded through the monitored metal sheet and the model predictions. The pattern at mid-day was due to the combined effect of solar radiation, exterior wind speed and air movement inside the gap as was previously explained. The real movement of the air inside the chamber is mainly conditioned geometrically by the presence of bolts, joints, structural reinforcements, etc Values, reported both theoretically and through experimentation, were compared to those obtained through the traditional McAdams formulation of the external convection coefficient [52], given by eq. (6):

$$h_{ex} = 5.62 + 3.9\,V$$

where "V" represents the average wind speed surrounding the sheet.

The maximum deviation occurred during the day with maximum differences of about 4 °C. At night this variation was reduced to (1-2 °C), which can be considered negligible. Similar outcomes were observed for a waste range of days across the whole campaign of measured data [53–55].

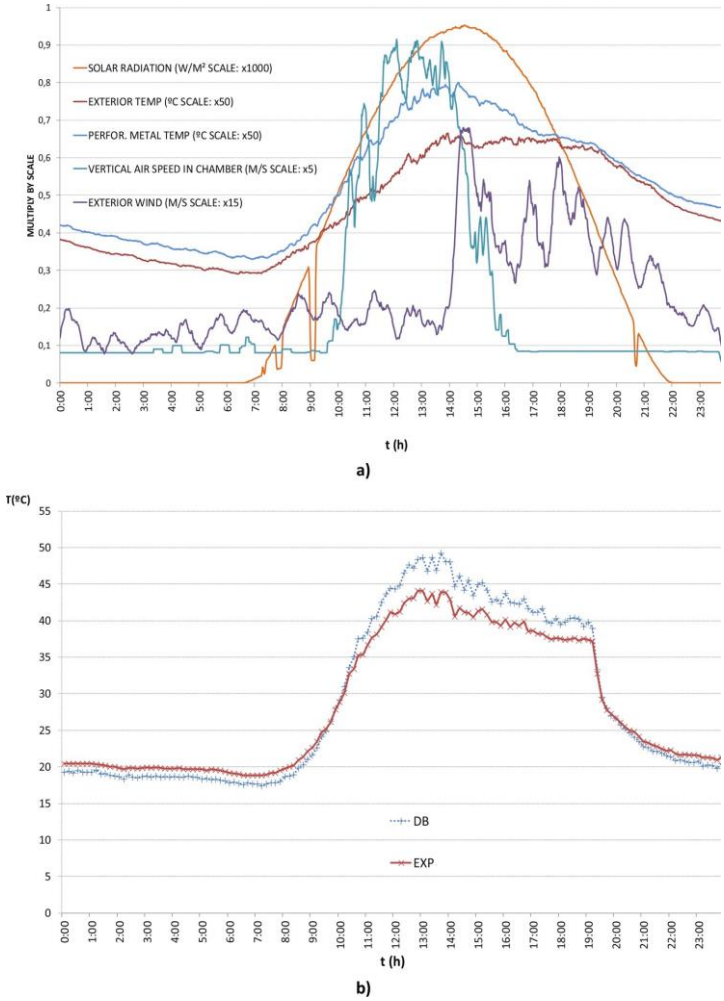


**Fig. 7.** Evolution of different outputs for a 24h day type, (a) temperatures of air and sheets, solar radiation and wind speed directly measured, and (b) comparative test between the temperatures of the metal sheet obtained through design builder (DB) and through direct measurement (EXP), for validation purposes.

*5.3. Complementary study with the infrared thermography (IRT) technique*

Infrared thermography analysis was implemented just to provide additional support to the data obtained by direct measurement. The outputs are coincident with the measured temperatures obtained for exactly the same external conditions (same day of reference), according to the previously defined procedure, with minimum deviations as will be shown later. The infrared thermography method is commonly usedto detect pathologies when analysing thermal behaviour of screens [56], for determining thermal losses [57,58] including air infiltrations through façades [59]. Table 6 shows the main features of the professional infrared camera ©TESTO 875-1i, equipped with automatic detection of hot and cool points and focused on industrial applications and buildings.

**Table 6** Main features of the "Testo 875-1i" infrared camera

| Testo 875-1i features | Value |
|---|---|
| Thermal sensitivity (NETD) | < 50 mK to 30 °C |
| Thermal sensitivity | 0.05 °C |
| Measurement range | −30 to +350 °C |
| Lents | 32° x 23° |
| Software | TESTO IRSoft |
| Thermal sensitivity (NETD) | < 50 mK to 30 °C |

The expression NETD stands for "Noise Equivalent Temperature Difference" [60–62]. It is a measure of how reliable a thermal imaging detector can distinguish between very small differences in thermal radiation. The camera must be pointed at a temperature controlled black body. The black body needs to be stabilized before starting the measurement [63]. The NETD is then measured at a specific temperature. It is not a single snapshot measurement, but rather a temporal measurement of noise.

The infrared camera calibration procedure [64–66] was performed in laboratory through direct measurement of particular set points by means of thermocouples placed on both sides of a sample corresponding to an identical perforated metal sheet, previously heated, as was depicted on Fig. 8a, while Fig. 8b shows a detailed thermography image for four set points. Experimental values compared for both internal and external sides of the perforated sheet, are shown in Table 7, demon strating a fully admissible calibration procedure.

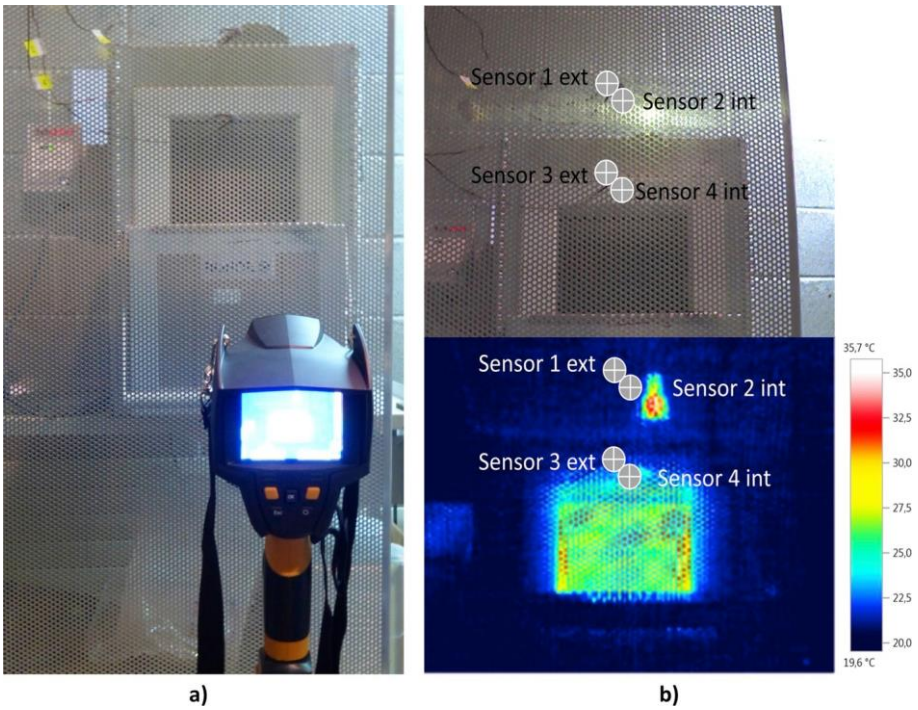


**Fig. 8.** Calibration procedure of the infrared camera, (a) through a sample in an experimental test bench, and (b) detailed thermograph image obtained for perforated metal sheet

**Table 7** Calibration of the infrared camera through direct measurement

| | $T_{exp}$ [°C] | $T_{tg.}$ [°C] |
|---|---|---|
| S1 ext | 30.50 | 30.65 |
| S2 int | 29.00 | 29.15 |
| S3 ext | 31.70 | 31.85 |
| S4 int | 31.50 | 31.60 |

Fig. 9a shows the thermography image obtained at medium distance (around 20 m) for the case study corresponding to the south-oriented perforated screen, in which the general behavior of the three lower floors can be observed in detail. Sensor placements correspond to the previously defined layout as was depicted in Fig. 5b. The higher temperatures reached on the open rectangle on the lower-left without the metallic envelope contrast as a clear indication of the protective effect on the envelope. In Fig. 9b, a picture of the upper part of the façade is depicted, revealing the uniform temperature distribution across the perforated sheets for the whole area. Finally, Fig. 9c shows a top view taken from the building roof towards the street, showing the thermal behavior of the air chamber (gap) walls, composed by the internal side of the sheets and the façade itself. The white colors shown on the lefthand side of the thermograph image reveal once again the effect of the upper rectangle shaped opening (see previous Fig. 5a (left)), which is directly exposed to the sunlight. Temperatures in general terms presented a uniform variability inside the gap with regard to the previously measured [67,68] due to a combined effect of the irregular geometry inside the chamber, responsible for additional buoyancydriven airflow, whose effects will be carefully addressed in a forthcoming work.

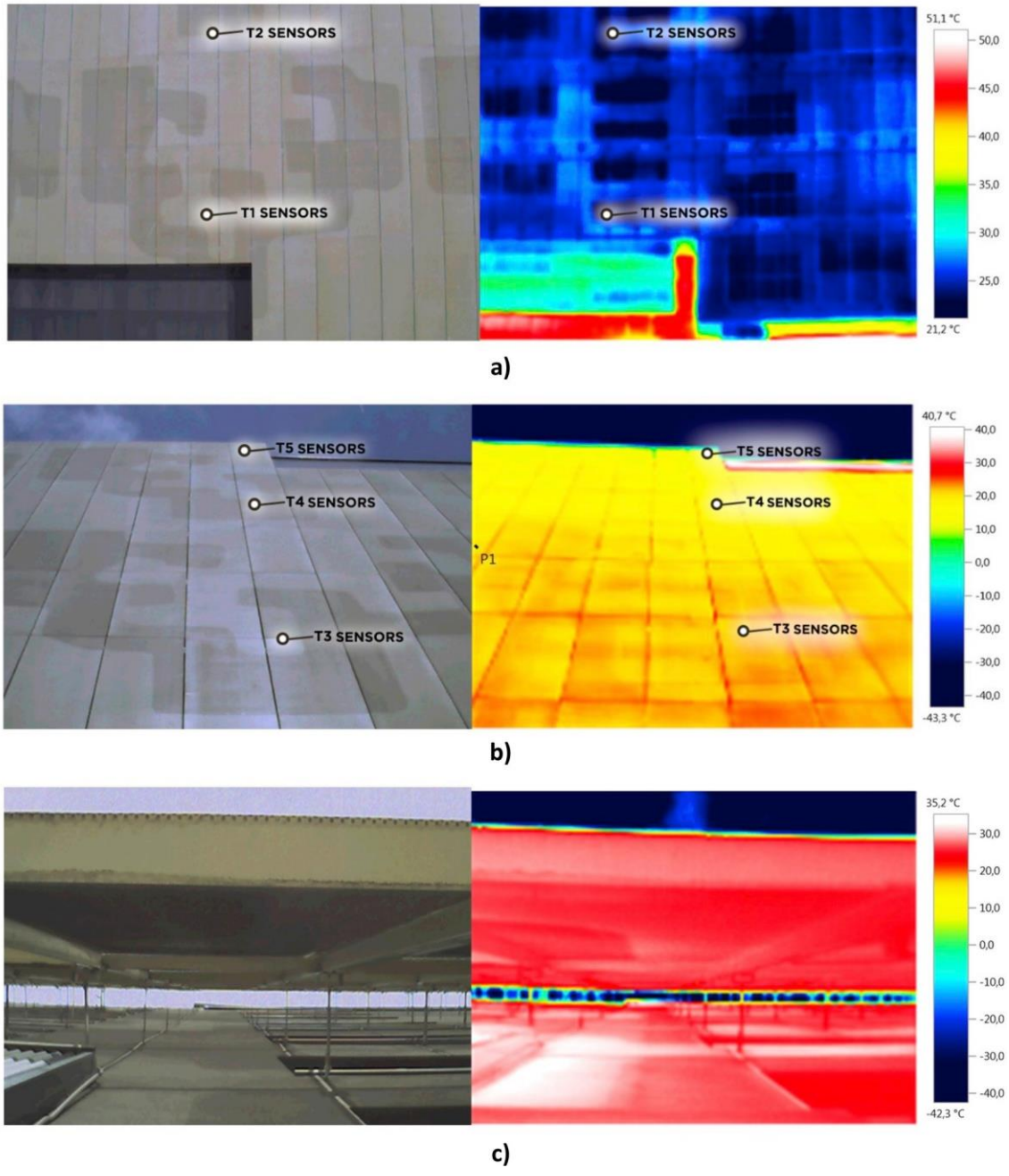


**Fig. 9.** Thermograph images (right) obtained from the corresponding perforated façade (left) for the same day type for validation purposes, (a) corresponding to the first three floors showing detailed thermal behavior of the sheets, (b) showing general thermal behavior of the whole façade, and (c) top view showing thermal behavior of the air chamber (gap).

5.4. Error treatment

Error treatment was performed through the square of the Pearson correlation coefficient ($R^2$), calculated using Equation (7) between the measured and predicted data values of the dependent variable, providing a measure of how well observed outcomes are replicated by the model, based on the proportion of total variation of outcomes.

Fig. 10 plots the temperature differences for the perforated sheets over the data predicted (X) both with the Design-Builder model (DB)and the Infrared thermography technique (TG) against the measured data (M) acquired through experimental test (EXP), respectively, for exactly the same period of time. The values obtained for $R^2$ were fully admissible in both cases, although the figures for the thermography analysis presented some slight differences with the measured values, due mainly to the heterogeneous geometry inside the gap [69,70]. It presents a lot of eye bolts, joint clips and moorings to fasten all the sheets with the added difficulty of the viscous effects around these particular items for really capturing the heat effect, due to reduced air passages between sheets along the whole façade [71–74].

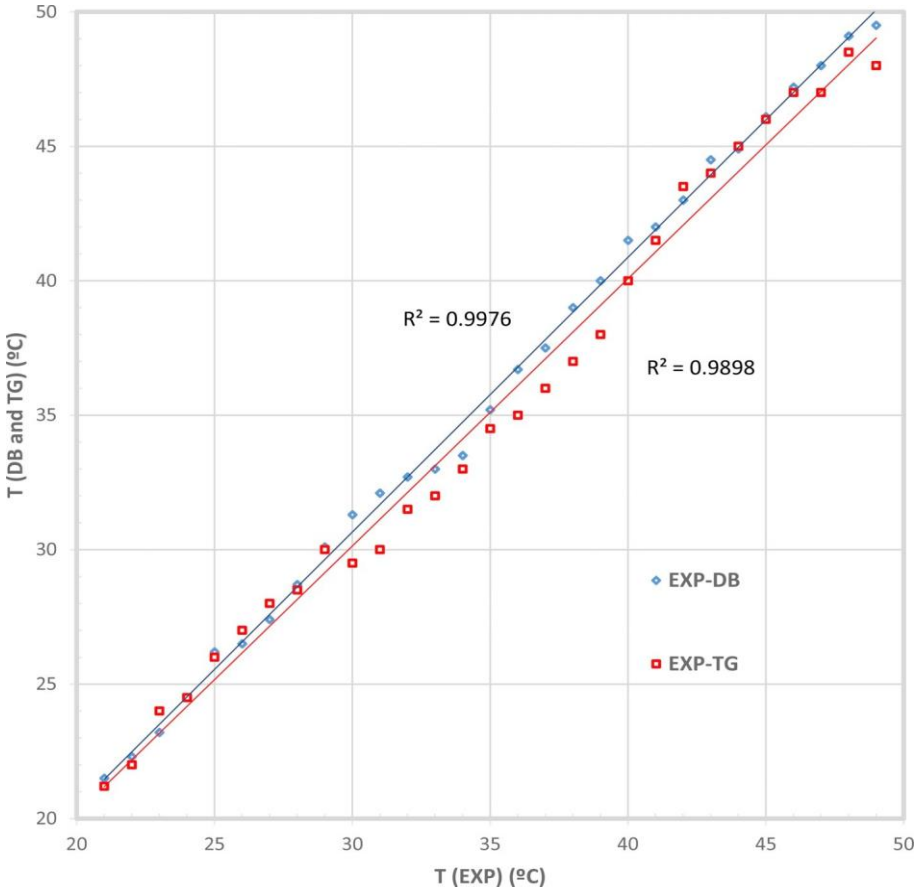


**Fig. 10.** Error estimation through the square of the Pearson product moment correlation coefficient ($R^2$).

## 6. Results and discussion

The case study in Spain addressed energy consumption and savings when implementing these shading constructive solutions in two different climate zones: I and V [50], represented by Bilbao and Seville, respectively, considering all the orientations according to the previously defined cardinal directions (see previous Fig. 4), for both of them, and taking into account different perforation rates. Table 8a shows the monthly averaged climate data characterization for zone I whereas Table 8b shows the same parameters for zone V [50], althoughit has to be noticed that Design Builder® takes the amount of radiationat any time of day into account and calculates the total addition of these gains [75–77].

Fig. 11 shows a comparative test on energy consumption (kWh/ year), for the abovementioned climatic zones, I (left) and V (right), according to orientation and perforation rates, now detached in cooling, heating and illumination needs respectively. The range of perforation rates under study covers from 10% to 100%, representing the latest the hypothetical case without any metallic cover, aiming to compare results with the reference case of the building without envelope.

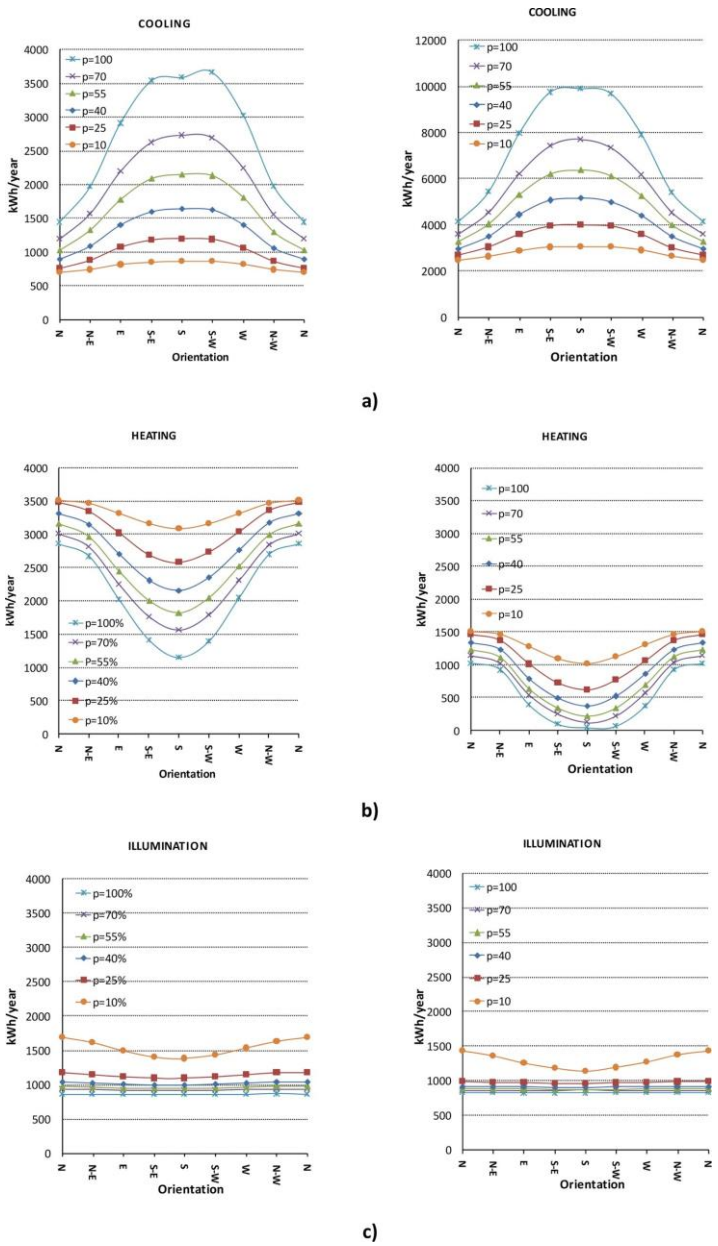


**Fig. 11.** Total energy consumption (kWh/year) according to the orientation and perforation rates for zone I (left) and zone V (right), detached in (a) cooling, (b) heating and (c) illumination loads

**Table 8** Monthly averaged climate data in Spain, (a) Zone I, and (b) Zone V

(a)

| Month | 1 | 2 | 3 | 4 | 5 | 6 | 7 | 8 | 9 | 10 | 11 | 12 |
|---|---|---|---|---|---|---|---|---|---|---|---|---|
| $I_r$ (kWh/m$^2$day) | 1.56 | 2.23 | 3.43 | 4.30 | 5.17 | 5.55 | 5.49 | 4.87 | 4.08 | 2.72 | 1.70 | 1.38 |
| $c_L$ (days/month) | 2.6 | 2.7 | 2.6 | 1.8 | 2.1 | 3.0 | 3.9 | 3.4 | 3.8 | 2.7 | 2.6 | 2.8 |
| R (mm) | 120 | 86 | 90 | 107 | 78 | 60 | 50 | 76 | 73 | 111 | 147 | 122 |
| $H_r$ (%) | 72 | 69 | 68 | 69 | 69 | 70 | 71 | 72 | 71 | 71 | 73 | 72 |
| $T_{min}$ (°C) | 5.1 | 5.1 | 6.4 | 7.6 | 10.6 | 13.4 | 15.4 | 15.7 | 13.8 | 11.4 | 8.1 | 5.9 |
| $T_{max}$ (°C) | 13.4 | 14.3 | 16.5 | 17.6 | 20.8 | 23.4 | 25.4 | 26.0 | 24.6 | 21.4 | 16.6 | 13.9 |
| $T_{avg}$ (°C) | 9.3 | 9.7 | 11.5 | 12.6 | 15.7 | 18.4 | 20.4 | 20.9 | 19.2 | 16.4 | 12.4 | 9.9 |

(b)

| Month | 1 | 2 | 3 | 4 | 5 | 6 | 7 | 8 | 9 | 10 | 11 | 12 |
|---|---|---|---|---|---|---|---|---|---|---|---|---|
| $I_r$ (kWh/m$^2$day) | 2.72 | 3.66 | 5.03 | 6.14 | 6.99 | 7.88 | 8.1 | 7.2 | 5.78 | 4.02 | 2.92 | 2.33 |
| $c_L$ (days/month) | 11.2 | 7.9 | 8.6 | 6.0 | 6.9 | 12.9 | 21.1 | 18.7 | 10.3 | 7.8 | 8.0 | 8.4 |
| R (mm) | 66 | 50 | 36 | 54 | 30 | 10 | 2 | 5 | 27 | 68 | 91 | 99 |
| $H_r$ (%) | 71 | 67 | 59 | 57 | 53 | 48 | 44 | 48 | 54 | 62 | 70 | 74 |
| $T_{min}$ (°C) | 5.7 | 7.0 | 9.2 | 11.1 | 14.2 | 18.0 | 20.3 | 20.4 | 18.2 | 14.4 | 10.0 | 7.3 |
| $T_{max}$ (°C) | 16.0 | 18.1 | 21.9 | 23.4 | 27.2 | 32.2 | 36.0 | 35.5 | 31.7 | 26.0 | 20.2 | 16.6 |
| $T_{avg}$ (°C) | 10.9 | 12.5 | 15.6 | 17.3 | 20.7 | 25.1 | 28.2 | 27.9 | 25 | 20.2 | 15.1 | 11.9 |

The most significant outputs represented by the **cooling** needs of the building, are due to the solar radiation. Obviously the higher thesolar radiation, the greater the cooling requirements, especially in zones characterized by higher averaged irradiance values, such as zone V, in which the south related façades represent the highest penalization rates in terms of cooling needs, as can be seen in Fig. 11a, with peak annual values between 750 and 3,700 kW h/year for zone I (left) depending on the perforation rate, whereas much higher figures were reached for zone V (right) between 2,300 and 10,000 kW h/year for the same configurations. It should also highlighted that the scale is different in both cases, due to the great difference in solar radiation loads between the two abovementioned zones.

Regarding the heating loads (Fig. 11b) the situation is reversed, as the closer the façade is oriented towards the south, the lower the energy consumption that is needed for heating purposes, which was even lower for zone V (right) than for zone I (left), as expected. Peak values were oscillating between 0 and 1,500 kW h/year for zone V whereas in zone I values between 1,200 and 3,500 kW h/year were reached, so the North represents the most unfavourable orientation.

Finally, regarding illumination requirements, the outputs obtained for both zones resulted rather similar, as depicted in Fig. 11c, with values oscillating around 900 and 1,700 kW h/year for zone I, whereas for zone V the values resulted slightly lower. Obviously, the lower the perforation rate, the greater the illumination load needed, due to the added shadow effect, especially meaningful for p = 10% in both cases. Aiming to show the effect over the total energy consumption of such enclosures (compared to the configuration of reference with no envelope) according to the orientation, two of the previously mentioned configurations of perforation rates were selected, corresponding to the optimum design ranges for zones I and V (40% and 10% respectively), as reported in Ref. [8]. It has to be highlighted that from this previousstudy, the optimal perforation rate for zone V taking in account only the solar radiation was p = 10%, but due to the visual concerns previously referred into this present study as a result of its dense shading rate, the value of p = 25% was finally adopted as the optimum for this particular zone.

Fig. 12 shows, in a spider web graph, a comparative test between the building without perforated metal sheet protection (100% of openings) and the optimized perforation rate for energy consumptions in each zone (40% for zone I Figure 12a and 25% for zone V respectively, Fig. 12b), according to façade orientations. As can be observed, the maximum oscillations for both zones always occurred towards the south, with larger relative differences, for zone V, of an order of magnitude of around five times than for zone I. The rest of the configurations for both scenarios would be placed in between those two polygonal curves.

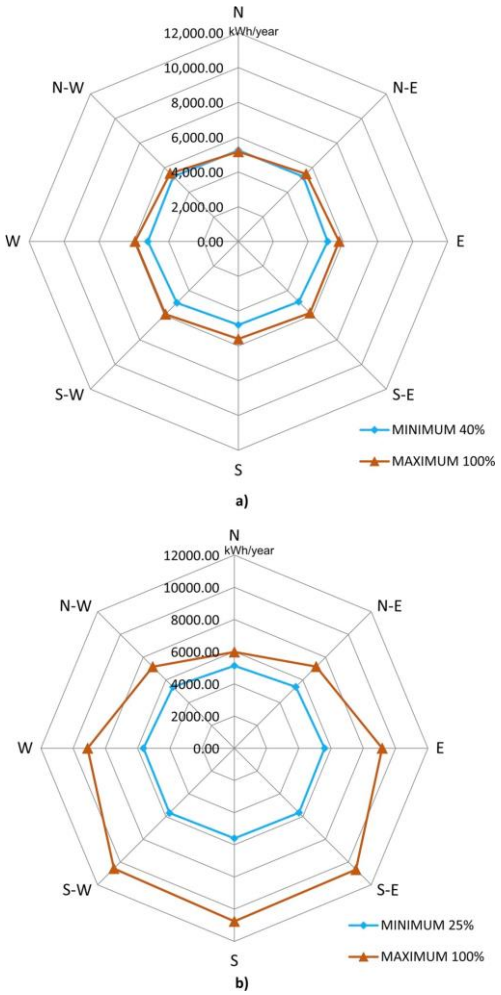


**Fig. 12.** Maximum and minimum energy consumption (kWh/year) according tothe façade orientation and the optimized perforation rates for (a) zone I, and (b) zone V

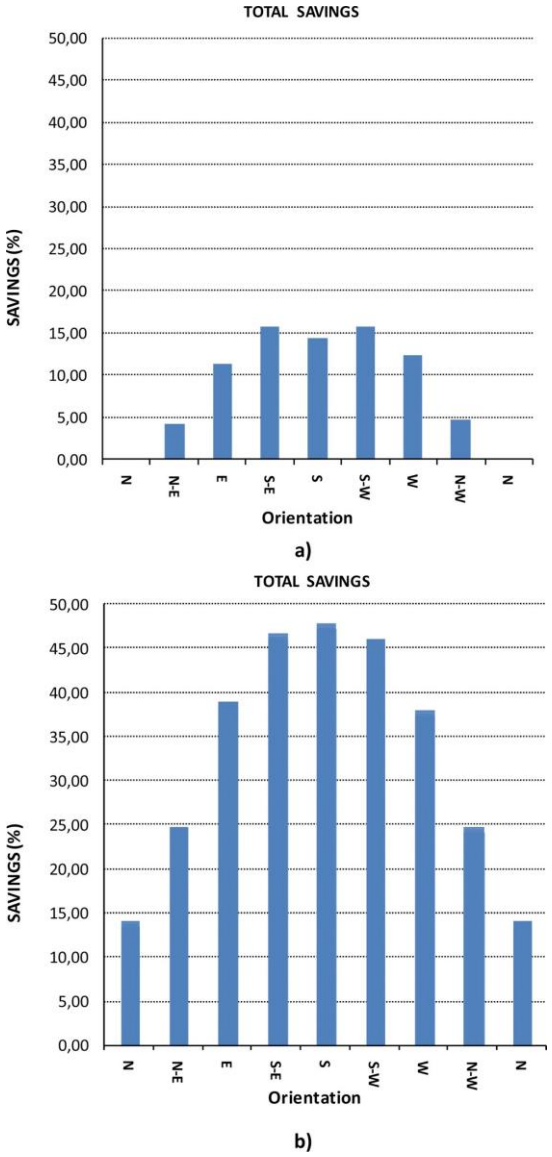


**Fig. 13.** Percentage of energy savings according to the façade orientation and location for optimal configurations, such as (a) p = 40% for zone I, and (b)p = 25% for zone V

Fig. 13a summarizes the percentage of total energy savings. For zone I, Fig. 13a, with the results plotted in the case of p = 40% (the optimal design for this zone), while Fig. 13b shows essentially the samefor zone V, plotted here at its optimal configuration of p = 25%. The closer to the south orientation, the greater the savings achieved, especially for zone V with peak values of 48% while significantly lower figures of around 15% were achieved for zone I for the same material and colour of the metal (galvanized steel) sheets that were tested. Neither of the two outcomes are negligible.

## 7. Conclusions

The main contribution of this research is its assessment of the influence of both orientation and latitude on the performance of double skin envelopes for buildings made by perforated sheets for different configurations. A survey on visual perception at short and long distances was administered to a population of more than 100 participants, inquiring into the different effects between the patterns. The main conclusion of this study revealed that the patterns with smaller hole diameters were best accepted over the shortest distance, but as this distance increased, the perception through the different patterns became more uniform.

A detailed analysis in different latitudes across Europe has taken 18 relevant cities into account, distributed along their various different parallels, through the "Ecotect®" software, demonstrating its suitability through a comparative test of energy gains, with and without the protective perforated screen, revealing great differences according to their location. This preliminary study was followed by the implementation of a numerical model for predicting the thermal behaviour

of these perforated screens, through the Energyplus®. The predictions were consistent with the values previously simulated by Ecotect® for the reference closure unit.

The energy study was based on the heat flow exchanged across the perforated screen, air-gap chamber and interior of the building, taking into account additional variables, such as location and orientation, and quantifying its influence on the total building load on annual basis under which the internal climate control system is operating. By way of example, the method was presented in detail for two rather different climate zones in Spain named respectively I (cold) and V (hot). It was finally validated both through an extensive test campaign carried outover a south-oriented façade and through the thermography technique, showing remarkable matches with the numerical outputs previously obtained.

The behaviour of such screens according to the different orientations, was finally addressed through three different figures (cooling, heating and illumination needs), which in some cases, are very relevant, especially the cooling needs of the building, reporting oscillations of around 6,000 kW h/year (for zone V), between north and south location for optimal configurations, such as (a) p = 40% for zone I, and (b) p = 25% for zone V orientations, while both heating and illumination needs were significantly lower, especially for zone V.

Taking into account that this former factor, “cooling”, is the most relevant one regarding energy consumption, as discussed, and even though this reduction in cooling consumption for zone V was of a larger order of magnitude, the conclusions of this study are that the implementation of these particular perforated screens, are in fact really useful in terms of energy demand reductions in the buildings.

With regard to the location, savings of up to 900 kW h/year for zoneI and 5,000 kW h/year for zone V can be achieved, for south oriented optimal configurations in both cases For those optimized combinations of perforation rates, savings of as much as 15% in energy consumption for the coldest areas, and around 48% for the hottest ones, were achieved, which are by no means negligible values.

Finally, other shading devices have been used were presented in literature, such as different external blind combinations or internal shading devices. Further comparative testing on energy gains between perforated screens and these devices will be addressed in an upcoming work.

**Acknowledgements**

The authors are deeply grateful to the Basque Government, through projects IT781-13 and IT1314-19, and to all those involved in the different stages for their guidance and invaluable help at all times in the arduous process of model validation. This research did not receive any specific grant from funding agencies in the public, commercial, or notfor-profit sectors.

**References**

[1] E. Diaz Lozano, J.A. Siegel, Indoor environmental quality in social housing: a lit- erature review, Build. Environ. 131 (2018) 231–241.
[2] A. Roetzel, A. Tsangrassoulis, Impact of climate change on comfort and energy performance in offices, Build. Environ. 57 (2012) 349–361.
[3] N. Nazarian, J.A. Acero, L. Norford, Outdoor thermal comfort autonomy: perfor- mance metrics for climate conscious urban design, Build. Environ. 155 (2019) 145–160.
[4] G. Vox, I. Blanco, E. Schettini, Green façades to control wall surface temperature inbuildings, Build. Environ. 129 (2018) 154–166.
[5] C.M. Lai, S. Hokoi, Solar façades: a review, Build. Environ. 91 (2015) 152–165.
[6] I. Konstantzos, A. Tzempelikos, Y.C. Chan, Experimental and simulation analysis of daylight glare probability in offices with dynamic window shades, Build. Environ. 87 (2015) 244–254.
[7] L.C.O. Souza, H.A. Souza, E.F. Rodrigues, Experimental and numerical analysis of a naturally ventilated double-skin façade, Energy Build. 165 (2018) 328–339.
J.M. Blanco, P. Arriaga, E. Rojí, J. Cuadrado, Investigating the thermal behavior ofdouble-skin perforated sheet façades: Part A: model characterization and validationprocedure, Build. Environ. 82 (2014) 50–62.
[8] M. David, M. Donn, F. Garde, A. Lenoir, Assessment of the thermal and visual ef- ficiency of solar shades, Build. Environ. 46/7 (2011) 1489–1496.
[9] K. Konis, Evaluating daylighting effectiveness and occupant visual comfort in a side- lit open-plan office building in San Francisco, California, Build. Environ. 59 (2013) 662–677.
[10] S.M. Hosseini, M. Mohammadi, A. Rosemann, T. Schröder, J. Lichtenberg, A mor- phological approach for kinetic façade design process to improve visual and thermal comfort: Review, Build. Environ. 153 (2019) 186–204.
[11] M. Bessoudo, A. Tzempelikos, A.K. Athienitis, R. Zmeureanu, Indoor thermalenvironmental conditions near glazed facades with shading devices Part I: ex- periments and building thermal model, Build. Environ. 45/11 (2010) 2506–2516.
[12] J. Ivanovic-Sekularac, J. Cikic-Tovarovic, N. Sekularac, Application of wood as an element of façade cladding in construction and reconstruction of architectural ob- jects to improve their energy efficiency, Energy Build. 115 (2016) 85–93.
[13] H. Shen, A. Tzempelikos, Sensitivity analysis on daylighting and energy perfor- mance of perimeter offices with automated shading, Build. Environ. 59 (2013) 303–314.
[14] T. Ihara, B. Jelle, T. Gao, A. Gustavsen, Accelerate aging of treated aluminum or useas a cool colored material for façades, Energy Build. 112 (2016) 184–197.
[15] B. Pelaz, J.M. Blanco, J. Cuadrado, Z. Egiluz, A. Buruaga, Analysis of the influence of wood cladding on the thermal behavior of building façades; characterizationthrough simulation by using different tools and comparative testing validation,Energy Build. 141 (2017) 349–360.
[16] E. Vereecken, S. Roels, Wooden beam ends in combination with interior insulation: an experimental study on the impact of convective moisture transport, Build. Environ. 148 (2019) 524–534.
[17] M. Manso, J. Castro-Gomes, Green wall systems: a review of their characteristics,Renew. Sustain. Energy Rev. 41 (2015) 863–871.
[18] K. Gunawardena, K. Steemers, Living walls in indoor environments, Build. Environ. 148 (2019) 478–487.
[19] N. Hashemi, R. Fayaz, M. Sarshar, Thermal behaviour of a ventilated double skin facade in hot arid climate, Energy Build. 42 (2010) 1823–1832.
[20] C. Lamnatou, J.D. Mondol, D. Chemisana, C. Maurer, Modelling and simulation of Building-Integrated solar thermal systems: behavior of the system, Renew. Sustain.Energy Rev. 45 (2015) 36–51.
[21] F. Bougiatioti, M. Aimilios, The architectural integration of active solar systems. Building applications in the eastern mediterranean region,

Renew. Sustain. EnergyRev. 47 (2015) 966–982.
[22] X. Zhang, J. Shen, Y. Lu, W. He, P. Xu, X. Zhao, Z. Qiu, Z. Zhu, J. Zhou, X. Dong, Active Solar Thermal Façades (ASTFs): from concept, application to research questions, Renew. Sustain. Energy Rev. 50 (2015) 32–63.
[23] G. Cattarin, F. Causone, A. Kindinis, L. Pagliano, Outdoor test cells for building envelope experimental characterization a literature review, Renew. Sustain. Energy Rev. 54 (2016) 606–625.
[24] F. Marques, M.G. Gomes, A. Rodrigues, Measuring and estimating airflow in naturally ventilated double skin façades, Build. Environ. 87 (2015) 292–301.
[25] A. Kirimtat, B. KundakciKoyunbaba, I. Chatzikonstantinou, S. Sariyildiz, Review of simulation modeling for shading devices in buildings, Renew. Sustain. Energy Rev. 53 (2016) 23–49.
[26] P.K. Heiselberg, Integrating environmentally responsive elements in buildings: new ECBCS research project (Annex 44), ECBCS News (39) (2004) 6–7.
[27] Ecotect Analysis Sustainable Building Design Software Autodesk. (last accessed 2019-02-29).
[28] EnergyPlus, Engineering Reference Manual, Building Technologies Program, USDepartment of Energy (DOE), 2014.
[29] A. Kylili, P.A. Fokaides, P. Christou, S.A. Kalogirou, Infrared thermography (IRT) applications for building diagnostics: a review, Appl. Energy 134 (2014) 531–549.
[30] J.P. Aguerrea, R. Nahon, E. Garcia-Nevado, C. La Borderie, E. Fernandez, B. Beckers, A street in perspective: thermography simulated by the finite elementmethod, Build. Environ. 148 (2019) 225–239.
[31] M. Fox, D. Coley, S. Goodhew, P. deWilde, Thermography methodologies for de- tecting energy related building defects, Renew. Sustain. Energy Rev. 40 (2014) 296–310.
[32] D. Bienvenido-Huertas, J. Bermúdez, J.J. Moyano, D. Marín, Influence of ICHTC correlations on the thermal characterization of façades using the quantitative in- ternal infrared thermography method, Build. Environ. 149 (2019) 512–525.
[33] J.H.K. Lai, F.W.H. Yik, Perception of importance and performance of the indoor environmental quality of high-rise residential buildings, Build. Environ. 44 (2009) 352–360.
[34] Y.A. Horr, M. Arif, A. Kaushik, A. Mazroei, M. Katafygiotou, E. Elsarrag, Occupant productivity and office indoor environment quality: a review of the literature, Build. Environ. 105 (2016) 369–389.
[35] G.Y. Yun, H.J. Kong, H. Kim, J.T. Kim, A field survey of visual comfort and lightingenergy consumption in open plan offices, Energy Build. 46 (2012) 146–151.
[36] F. Sicurella, G. Evola, E. Wurtz, A statistical approach for the evaluation of thermaland visual comfort in free-running buildings, Energy Build. 47 (2012) 402–410.
[37] Y. Geng, W. Ji, B. Lin, Y. Zhu, The impact of thermal environment on occupant IEQperception and productivity, Build. Environ. 121 (2017) 158–167.
[38] W. O'Brien, I. Gaetani, S. Carlucci, P.J. Hoes, J.L.M. Hensen, On occupant-centric building performance metrics, Build. Environ. 122 (2017) 373–385.
[39] N. Djongyang, R. Tchinda, D. Njomo, Thermal comfort: a review paper, Renew. Sustain. Energy Rev. 14 (2010) 2626–2640.
[40] D. Vakalis, M. Touchie, E. Tzekova, H.L. MacLean, J.A. Siegel, Indoor environ- mental quality perceptions of social housing residents, Build. Environ. 150 (2019) 135–143.
[41] D. Crawley, L. Lawrie, F. Winkelmann, W. Buhl, Y.J. Huang, C. Pedersen, R. Strand, R. Liesen, D. Fisher, M. Witter, J. Glazer, EnergyPlus: creating a new generation building energy simulation program, Energy Build. 33/4 (2001) 443–457.
[42] H. Yi, R.S. Srinivasan, W.W. Braham, An integrated energy emergy approach to building form optimization: use of EnergyPlus, emergy analysis and Taguchi-re- gression method, Build. Environ. 84 (2015) 89–104.
[43] J.M. Blanco, A. Buruaga, E. Rojí, J. Cuadrado, Energy assessment and optimization of perforated metal sheet double skin façades through Design Builder; A case study in Spain, Energy Build. 111 (2016) 326–336.
[44] H. Simmler, B. Binder, Experimental and numerical determination of the total solar energy transmittance of glazing with Venetian blind shading, Build. Environ. 43/2 (2008) 197–204.
[45] B.J. Futrell, E.C. Ozelkan, D. Brentrup, Bi-objective optimization of building en- closure design for thermal and lighting performance, Build. Environ. 92 (2015) 591–602.
[46] S.A. Zaki, S.A. Damiati, H.B. Rijal, A. Hagishima, A.A. Razak, Adaptive thermal comfort in university classrooms in Malaysia and Japan, Build. Environ. 122 (2017)294–306.
[47] D.A. Chi, D. Moreno, J. Navarro, Design optimisation of perforated solar façades in order to balance daylighting with thermal performance, Build. Environ. 125 (2017) 383–400.
[48] Thermal Performance of Windows, Doors and Shading Devices-Detailed Calculations, ISO15099, 2001.
[49] Spain, Royal Decree 2429/1979 Approving the Basic Building Norm on Thermal Conditions in Buildings NBE-CT-79, (1979) Available at: https://www.boe.es/boe/ dias/1979/10/22/pdfs/A24524-24550.pdf , Accessed date: 8 March 2019.
[50] International Organization for Standardization, UNE EN ISO 6946:2012 BuildingComponents and Building Elements. Thermal Resistance and Thermal Transmittance, Calculation Method, 2012.
[51] W.H. McAdams, Heat Transmission, McGraw Hill, New York, 1954.
[52] F. Noris, G. Adamkiewicz, W.W. Delp, T. Hotchi, M. Russell, B.C. Singer, M. Spears, K. Vermeer, W.J. Fisk, Indoor environmental quality benefits of apartment energy retrofits, Build. Environ. 68 (2013) 170–178.
[53] F. Tahmasebi, A. Mahdavi, An inquiry into the reliability of window operation models in building performance simulation, Build. Environ. 105 (2016) 343–357.
[54] Á. Broderick, M. Byrne, S. Armstrong, J. Sheahan, A.M. Coggins, A pre and post evaluation of indoor air quality, ventilation, and thermal comfort in retrofitted cooperative social housing, Build. Environ. 122 (2017) 126–133.
[55] M. Fox, S. Goodhew, P. de Wilde, Building defect detection: external versus internal thermography, Build. Environ. 105 (2016) 317–331.
[56] A.M. O'Grady, A.A. Lechowska, A.M. Harte, Infrared thermography technique as an in-situ method of assessing heat loss through thermal bridging, Energy Build. 135 (2017) 20–32.
[57] I. Nardia, E. Lucchib, T. de Rubeis, D. Ambrosini, Quantification of heat energy losses through the building envelope: a stateof-the-art analysis with critical andcomprehensive review on infrared thermography, Build. Environ. 146 (2018) 190–205.
[58] C. Lerma, E. Barreira, R. Almeida, A discussion concerning active infrared ther- mography in the evaluation of buildings air infiltration, Energy Build. 168 (2018) 56–66.
[59] G. Dall'O, L. Sarto, A. Panza, Infrared screening of residential buildings for energy audit purposes: results of a field test, Energies 6 (2013) 3859–3878.
[60] H. Zhanga, R. Yanga, S. Youa, W. Zhenga, X. Zhenga, T. Yea, The CPMV index for evaluating indoor thermal comfort in buildings with solar radiation, Build. Environ.134 (2018) 1–9.
[61] A.M. O'Grady, A.A. Lechowska, A.M. Harte, Quantification of heat losses through building envelope thermal bridges influenced by wind velocity using the out-door infrared thermography technique, Appl. Energy 108 (2017) 1038–1052.
[62] B. Tejedor, M. Casals, M. Gangolells, Assessing the influence of operating conditions and thermophysical properties on the accuracy of in-situ measured U-values using quantitative internal infrared thermography, Energy Build. 171 (2018) 64–75.
[63] R. Albatici, A.M. Tonelli, M. Chiogna, A comprehensive experimental approach for the validation of quantitative infrared thermography in the evaluation of building thermal transmittance, Appl. Energy 141 (2015) 218–228.
[64] International Organization for Standardization, ISO/IEC Guide 98-3:2008. Uncertainty of Measurement. Part 3: Guide to the Expression of Uncertainty inMeasurement (GUM: 1995), (2008).
[65] V. Tzifa, G. Papadakos, A.G. Papadopoulou, V. Marinakis, J. Psarras, Uncertaintyand method limitations in a short-time measurement of the effective thermal transmittance on a building envelope using an infrared camera, Int. J. Sustain. Energy (2014) 1–19.
[66] H. Manz, A. Schaelin, H. Simmler, Airflow patterns and thermal behaviour of me- chanically ventilated glass double façades, Build. Environ. 39 (2004) 1023–1033.
[67] A. Pappas, Z. Zhai, Numerical investigation on thermal performance and correla- tions of double skin façade with buoyancy-driven airflow, Energy Build. 40 (2008) 466–475.
[68] F. Stazi, F. Tomassoni, A. Vegliò, C. di Perna, Experimental evaluation of ventilated walls with an external clay cladding, Renew. Energy 36 (2011) 3373–3385.
[69] N. Sánchez, E. Giancola, J. Suárez, E. Blanco, R. Heras, Experimental evaluation ofthe airflow behavior in horizontal and vertical Open Joint Ventilated Facades using Stereo-PIV, Renew. Energy 109 (2017) 613–623.

[70] S. Dactu, L. Ibos, Y. Candau, S. Matteï, Improvement of building wall surface temperature measurement by infrared thermography, Infrared Phys. Technol. 46 (2005) 451–467.
[71] J. Feijó-Muñoz, R.A. González-Lezcano, I. Poza-Casado, M.A. Padilla-Marcos, A. Meiss, Airtightness of residential buildings in the Continental area of Spain, Build. Environ. 148 (2019) 299–308.
[72] L. Vazquez, J.M. Blanco, R. Ramis, F. Peña, D. Diaz, Robust methodology for steady state measurements estimation based framework for a reliable long term thermal power plant operation performance monitoring, Energy 93 (2015) 923–944.
[73] J. Esarte, A. Bernardini, J.M. Blanco, R. Sancibrian, Optimizing the design for a two- phase cooling loop heat pipe Part A: numerical model, validation and application to a case study, Appl. Therm. Eng. 99 (2016) 892–904.
[74] C.A. de Gracia, L. Navarro, E. Oró, L.F. Cabeza, Numerical modelling of ventilated façades: a review, Renew. Sustain. Energy Rev. 22 (2013) 539–549.
[75] R. Zhang, K.P. Lam, S. Yao, Y. Zhang, Coupled EnergyPlus and computational fluid dynamics simulation for natural ventilation, Build. Environ. 68 (2013) 100–113.
[76] R. Hay, C.P. Ostertag, Life cycle assessment (LCA) of double-skin façade (DSF) system with fiber-reinforced concrete for sustainable and energy-efficient buildingsin the tropics, Build. Environ. 142 (2018) 327–341.